Hindawi
Shock and Vibration
Volume 2018, Article ID 7213606, 12 pages
https://doi.org/10.1155/2018/7213606

Research Article

Heteroclinic Bifurcation Behaviors of a Duffing Oscillator with Delayed Feedback

Shao-Fang Wen,[1] **Ju-Feng Chen**,[2] **and Shu-Qi Guo**[3]

[1]*Department of Traffic and Transportation, Shijiazhuang Tiedao University, Shijiazhuang 050043, China*
[2]*Department of Mathematics and Physics, Shijiazhuang Tiedao University, Shijiazhuang 050043, China*
[3]*Department of Engineering Mechanics, Shijiazhuang Tiedao University, Shijiazhuang 050043, China*

Correspondence should be addressed to Shao-Fang Wen; wsf39811@163.com

Received 17 July 2017; Revised 22 November 2017; Accepted 21 December 2017; Published 21 January 2018

Academic Editor: Gianluca Gatti

The heteroclinic bifurcation and chaos of a Duffing oscillator with forcing excitation under both delayed displacement feedback and delayed velocity feedback are studied by Melnikov method. The Melnikov function is analytically established to detect the necessary conditions for generating chaos. Through the analysis of the analytical necessary conditions, we find that the influences of the delayed displacement feedback and delayed velocity feedback are separable. Then the influences of the displacement and velocity feedback parameters on heteroclinic bifurcation and threshold value of chaotic motion are investigated individually. In order to verify the correctness of the analytical conditions, the Duffing oscillator is also investigated by numerical iterative method. The bifurcation curves and the largest Lyapunov exponents are provided and compared. From the analysis of the numerical simulation results, it could be found that two types of period-doubling bifurcations occur in the Duffing oscillator, so that there are two paths leading to the chaos in this oscillator. The typical dynamical responses, including time histories, phase portraits, and Poincare maps, are all carried out to verify the conclusions. The results reveal some new phenomena, which is useful to design or control this kind of system.

1. Introduction

It is well known that many kinds of nonlinearities exist in engineering systems, such as parametric excitation, nonsmoothness, time delay, discontinuity, and large deformation [1–6]. These nonlinearities will make the system responses more complicated and the system performance deteriorated. In recent years, the complicated dynamics of typical nonlinear systems have been more and more concerned. Duffing oscillator is one of the most common and typical models in nonlinear dynamical systems. Among these nonlinear systems the well-known Duffing oscillator is quite suitable to model the large deformation structure in many physics and engineering fields [7–10]. Moreover, time delay is an unavoidable and very common problem when those systems were controlled. It can influence the system dynamical characteristic and even destroy the system stability [11, 12]. The complicated Duffing nonlinear system with time delay is possible to generate more complex bifurcation and chaotic dynamic phenomena [11–14]. For example, Luo [15] studied the bifurcation trees of time-delay Duffing oscillator by a semianalytical method. Amer et al. [16] investigated the Duffing oscillator with parametric excitation under time-delay feedback based on the multiple scales perturbation method and analyzed the influences of the system parameters. Ji and Leung [17] studied the bifurcation control of a Duffing oscillator with parametrical excitation by a linear time-delayed feedback and discovered that the stable region could be broadened through choosing an appropriate feedback control. Zhang et al. [18] investigated the multipulse global bifurcations and chaotic behaviors of a cantilever beam by extended Melnikov method. Theodossiades and Natsiavas [19] and Van Dooren [20] studied the period-doubling bifurcations for gear-pair systems with periodic stiffness and backlash. Rusinek et al. [21, 22] investigated the dynamics of the time-delay Duffing oscillator. Besides,

they also studied the chaos and feedback control of the time-delay Duffing system and found the suitable time delay and feedback gain would destroy the chaotic attractor for Duffing system. Nana Nbendjo et al. [23] studied the effects of the control parameters in a double-well Duffing oscillator with the time delay by Melnikov theory.

The heteroclinic bifurcation and chaos behaviors are two of the most important characteristics in nonlinear dynamical systems. Many scholars paid attention to the heteroclinic bifurcation and chaos phenomena of nonlinear Duffing oscillator [24–26]. For example, Yang and Sun et al. [27, 28] investigated the necessary condition for the generating chaos of a double-well Duffing oscillator with bounded noise excitations and time-delay feedback by Melnikov theory. Siewe et al. [29] investigated the necessary condition for chaotic behavior of Duffing-Rayleigh system based on Melnikov theory. Cao et al. [30] presented a novel construction of homoclinic and heteroclinic orbits for nonlinear systems with a perturbation-incremental method. Chen and Yan [31] studied the heteroclinic bifurcation behavior in the Duffing-VDP oscillator by the hyperbolic Lindstedt-Poincare method and obtained the analytical heteroclinic solution. Chacon [32] and Maki et al. [33] investigated heteroclinic bifurcation phenomenon for different types of nonlinear systems based on Melnikov method, respectively. Lei and Zhang [34] investigated the chaotic motion of the Duffing system and came to the conclusion that the threshold for generating chaos could be changed by choosing the internal parameters of trichotomous noise.

All the above analyses mainly focused on qualitative, numerical, or simplified analytical solutions about the necessary condition for generating chaos. In this paper, the first-order exact analytical solution of the necessary condition for generating chaos in sense of Smale horseshoes in a Duffing oscillator with both delayed displacement feedback and delayed velocity feedback is obtained based on Melnikov theory. Besides, the numerical heteroclinic bifurcation results were presented and some new phenomena were found in the Duffing oscillator with time-delay feedback. The basic structure of this paper is arranged as follows. The Melnikov function is obtained based on Melnikov method, and the analytical necessary condition for generating chaos is also obtained in Section 2. In Section 3, the bifurcation curves and the largest Lyapunov exponents by numerical method are investigated. It can be found that there are two paths leading to chaos via period-doubling bifurcation in this system. Then the time histories, phase portraits, and Poincare maps with the typical system parameters are all presented to verify the new phenomenon. The influences of the delayed displacement and velocity feedback parameters on generating chaos are analyzed. The comparisons of the numerical results with the analytical results are also fulfilled in this section. Finally, the conclusions of this paper are summarized.

2. Analytical Necessary Condition for Chaos in Sense of Smale Horseshoes

Duffing oscillator is one of the most familiar systems in nonlinear dynamics. Under the function of both delayed displacement feedback and delayed velocity feedback, a Duffing oscillator with forcing excitation would be investigated in this section. The dynamic equation is

$$\ddot{x} + kx - \alpha x^3 + c\dot{x} = f\cos(\omega t) + ux(t-\tau_1) + v\dot{x}(t-\tau_2), \tag{1}$$

where k is the linear stiffness coefficient, α is nonlinear stiffness coefficient, c is linear damping coefficient, f and ω are excitation amplitude and frequency, respectively, u and v are displacement and velocity feedback coefficients, respectively, and τ_1 and τ_2 are time delays of displacement and velocity feedback, respectively. Here all the system parameters are positive and dimensionless.

Introducing the transformation

$$\begin{aligned} c &= \varepsilon c_1, \\ f &= \varepsilon f_1, \\ u &= \varepsilon u_1, \\ v &= \varepsilon v_1, \end{aligned} \tag{2}$$

where ε is a small real parameter, (1) turns into

$$\begin{aligned} &\ddot{x} + kx - \alpha x^3 \\ &\quad = \varepsilon\left[f_1\cos(\omega t) + u_1 x(t-\tau_1) + v_1\dot{x}(t-\tau_2) - c_1\dot{x}\right]. \end{aligned} \tag{3}$$

Supposing $\varepsilon = 0$, the unperturbed system is

$$\ddot{x} + kx - \alpha x^3 = 0. \tag{4}$$

There are three equilibrium points, where $(0, 0)$ is a center, and $(\pm\sqrt{k/\alpha}, 0)$ are two saddle points. Generally speaking, if the unperturbed system is conservative system and the number of saddle points is 1 larger than that of the centers, there may be heteroclinic orbit in this system. Here the heteroclinic orbit connecting the two saddle points satisfies the formula

$$\frac{1}{2}\dot{x}^2 + \frac{k}{2}x^2 - \frac{\alpha}{4}x^4 = \frac{k^2}{4\alpha}. \tag{5}$$

Supposing $x = 0$ at $t = 0$, the calculating result is

$$\dot{x}_0 = \pm\frac{k}{\sqrt{2\alpha}}. \tag{6}$$

Integrating (5), one could obtain

$$\int_0^x \frac{\mathrm{d}x}{\pm\sqrt{k^2/2\alpha - kx^2 + (\alpha/2)x^4}} = t. \tag{7}$$

Calculating (7), it yields

$$x^{\pm}(t) = \pm\sqrt{\frac{k}{\alpha}}\tanh\left(\sqrt{\frac{k}{2}}t\right). \tag{8}$$

So (3) can be rewritten as

$$\dot{\vec{x}} = \vec{f}\left(\vec{x}\right) + \varepsilon \vec{g}\left(\vec{x}, t\right), \tag{9a}$$

where

$$\vec{x} = \begin{pmatrix} x_1 \\ x_2 \end{pmatrix} = \begin{pmatrix} x \\ \dot{x} \end{pmatrix}, \tag{9b}$$

$$\vec{f}\left(\vec{x}\right) = \begin{pmatrix} x_2 \\ -kx_1 + \alpha x_1^3 \end{pmatrix}, \tag{9c}$$

$$\vec{g}\left(\vec{x}, t\right) = \varepsilon \begin{bmatrix} 0 \\ -c_1 x_2 + f_1 \cos\left(\omega t\right) + u_1 x_1\left(t - \tau_1\right) + v_1 x_2\left(t - \tau_2\right) \end{bmatrix}. \tag{9d}$$

Then one can establish the heteroclinic orbit as follows:

$$x_1^{\pm}(t) = \pm\sqrt{\frac{k}{\alpha}} \tanh\left(\sqrt{\frac{k}{2}} t\right), \tag{10a}$$

$$x_2^{\pm}(t) = \pm\frac{k}{\sqrt{2\alpha}} \operatorname{sech}^2\left(\sqrt{\frac{k}{2}} t\right). \tag{10b}$$

Melnikov theory [35], proposed by Melnikov, is a perturbation method originally for proving the existence of transverse homoclinic or heteroclinic orbits. Melnikov theory has been applied in many researches. The Melnikov technique was firstly applied to study a periodically driven Duffing oscillator by Holmes [36]. The Melnikov technique is also valid in time-delay systems, which was proved in [37]. According to Melnikov theory, the perturbed function must be a periodicity of function. In (9a), the perturbed function $\vec{g}(\vec{x}, t)$ with time delay is also a periodic function which is satisfied with the basic condition of Melnikov theory. Therefore, many scholars have studied the dynamical characteristics of the time-delay Duffing system by Melnikov theory such as [23, 27, 28, 37]. All the existing analyses were mainly focused on qualitative, numerical, or simplified analytical solutions about the necessary condition for generating chaos. Here, Melnikov method is also applied to yield the Melnikov function as follows:

$$\begin{aligned} M\left(t_0\right) &= \vec{f}\left(\vec{x}\right) \wedge \vec{g}\left(\vec{x}, t\right) = \varepsilon \int_{-\infty}^{\infty} x_2^{\pm}(t) \left[-c_1 x_2^{\pm}(t)\right. \\ &\quad + f_1 \cos\omega\left(t + t_0\right) + u_1 x_1^{\pm}\left(t - \tau_1\right) \\ &\quad \left. + v_1 x_2^{\pm}\left(t - \tau_2\right)\right] \mathrm{d}t = M_1\left(t_0\right) + M_2\left(t_0\right) \\ &\quad + M_3\left(t_0\right) + M_4\left(t_0\right), \end{aligned} \tag{11a}$$

where

$$M_1\left(t_0\right) = -\varepsilon c_1 \int_{-\infty}^{\infty} \left[x_2^{\pm}(t)\right]^2 \mathrm{d}t = -\frac{2\sqrt{2}\varepsilon c_1 k\sqrt{k}}{3\alpha}, \tag{11b}$$

$$M_2\left(t_0\right) = \mp\frac{\varepsilon k f_1}{\sqrt{2\alpha}} \int_{-\infty}^{\infty} \operatorname{sech}^2\left(\sqrt{\frac{k}{2}} t\right) \cos\omega\left(t + t_0\right) \mathrm{d}t. \tag{11c1}$$

Making use of the odevity of integrand, (11c1) becomes

$$\begin{aligned} M_2\left(t_0\right) &= \mp\frac{\varepsilon k f_1}{\sqrt{2\alpha}} \cos\left(\omega t_0\right) \int_{-\infty}^{\infty} \operatorname{sech}^2\left(\sqrt{\frac{k}{2}} t\right) \cos\left(\omega t\right) \mathrm{d}t \\ &= \mp\frac{2\varepsilon f_1 \pi\omega}{\sqrt{2\alpha}} \cos\left(\omega t_0\right) \operatorname{csch}\left(\frac{\pi\omega}{\sqrt{2k}}\right). \end{aligned} \tag{11c2}$$

And the other parts in (11a) are

$$\begin{aligned} M_3\left(t_0\right) &= \varepsilon u_1 \int_{-\infty}^{\infty} x_2^{\pm}(t)\, x_1^{\pm}\left(t - \tau_1\right) \mathrm{d}t = \frac{\varepsilon k\sqrt{k} u_1}{2\alpha} \\ &\quad \cdot \int_{-\infty}^{\infty} \operatorname{sech}^2\left(\sqrt{\frac{k}{2}} t\right) \tanh\left[\sqrt{\frac{k}{2}}\left(t - \tau_1\right)\right] \mathrm{d}t \\ &= \frac{\sqrt{2}\varepsilon k u_1}{2\alpha} \operatorname{csch}^2\left(\sqrt{\frac{k}{2}} \tau_1\right) \\ &\quad \cdot \left[\sqrt{2k}\tau_1 - \sinh\left(\sqrt{2k}\tau_1\right)\right], \end{aligned} \tag{11d}$$

$$\begin{aligned} M_4\left(t_0\right) &= \varepsilon v_1 \int_{-\infty}^{\infty} x_2^{\pm}(t)\, x_2^{\pm}\left(t - \tau_2\right) \mathrm{d}t = \frac{\varepsilon k^2 v_1}{2\alpha} \\ &\quad \cdot \int_{-\infty}^{\infty} \operatorname{sech}^2\left(\sqrt{\frac{k}{2}} t\right) \operatorname{sech}^2\left[\sqrt{\frac{k}{2}}\left(t - \tau_2\right)\right] \mathrm{d}t \\ &= \frac{\sqrt{2}\varepsilon k\sqrt{k} v_1}{\alpha} \operatorname{csch}^3\left(\sqrt{\frac{k}{2}} \tau_2\right) \\ &\quad \cdot \left[\sqrt{2k}\tau_2 \cosh\left(\sqrt{\frac{k}{2}} \tau_2\right) - 2\sinh\left(\sqrt{\frac{k}{2}} \tau_2\right)\right]. \end{aligned} \tag{11e}$$

Through the analysis of the above results, the necessary condition for generating chaos in sense of Smale horseshoes can be obtained as follows:

$$\begin{aligned} \frac{2\varepsilon f_1 \pi\omega}{\sqrt{2\alpha}} \operatorname{csch}\left(\frac{\pi\omega}{\sqrt{2k}}\right) &> \left| -\frac{2\sqrt{2}\varepsilon c_1 k\sqrt{k}}{3\alpha} + \frac{\sqrt{2}\varepsilon k u_1}{2\alpha} \right. \\ &\quad \cdot \operatorname{csch}^2\left(\sqrt{\frac{k}{2}} \tau_1\right) \left[\sqrt{2k}\tau_1 - \sinh\left(\sqrt{2k}\tau_1\right)\right] \\ &\quad + \frac{\sqrt{2}\varepsilon k\sqrt{k} v_1}{\alpha} \operatorname{csch}^3\left(\sqrt{\frac{k}{2}} \tau_2\right) \\ &\quad \left. \cdot \left[\sqrt{2k}\tau_2 \cosh\left(\sqrt{\frac{k}{2}} \tau_2\right) - 2\sinh\left(\sqrt{\frac{k}{2}} \tau_2\right)\right] \right|. \end{aligned} \tag{12}$$

Replacing the parameters in (12) with the original system parameters, one can get

$$\begin{aligned}\frac{2f\pi\omega}{\sqrt{2\alpha}}\operatorname{csch}\left(\frac{\pi\omega}{\sqrt{2k}}\right) > \Bigg|&-\frac{2\sqrt{2}ck\sqrt{k}}{3\alpha}+\frac{\sqrt{2}ku}{2\alpha}\\ &\cdot\operatorname{csch}^2\left(\sqrt{\frac{k}{2}}\tau_1\right)\left[\sqrt{2k}\tau_1-\sinh\left(\sqrt{2k}\tau_1\right)\right]\\ &+\frac{\sqrt{2}k\sqrt{k}v}{\alpha}\operatorname{csch}^3\left(\sqrt{\frac{k}{2}}\tau_2\right)\\ &\cdot\left[\sqrt{2k}\tau_2\cosh\left(\sqrt{\frac{k}{2}}\tau_2\right)-2\sinh\left(\sqrt{\frac{k}{2}}\tau_2\right)\right]\Bigg|.\end{aligned} \tag{13}$$

3. Numerical Simulation and Influences of Delayed Feedback on Bifurcation and Chaotic Behaviors

If the delayed displacement feedback coefficient u and velocity feedback coefficient v are all small enough, then (13) becomes

$$\begin{aligned}\frac{2f\pi\omega}{\sqrt{2\alpha}}\operatorname{csch}\left(\frac{\pi\omega}{\sqrt{2k}}\right) > &\frac{2\sqrt{2}ck\sqrt{k}}{3\alpha}-\frac{\sqrt{2}ku}{2\alpha}\\ &\cdot\operatorname{csch}^2\left(\sqrt{\frac{k}{2}}\tau_1\right)\left[\sqrt{2k}\tau_1-\sinh\left(\sqrt{2k}\tau_1\right)\right]\\ &-\frac{\sqrt{2}k\sqrt{k}v}{\alpha}\operatorname{csch}^3\left(\sqrt{\frac{k}{2}}\tau_2\right)\\ &\cdot\left[\sqrt{2k}\tau_2\cosh\left(\sqrt{\frac{k}{2}}\tau_2\right)-2\sinh\left(\sqrt{\frac{k}{2}}\tau_2\right)\right].\end{aligned} \tag{14}$$

Through the analysis of (14), we could find that the analytical necessary condition for generating chaos is influenced by the delayed displacement feedback and delayed velocity feedback, respectively. That is to say, the coupling relationship does not exist between delayed displacement feedback and delayed velocity feedback. According to the above analysis of the relationship between the two kinds of feedback, the influences of the two kinds of delayed feedback on bifurcation and chaos behaviors will be investigated separately in the following sections.

3.1. The Influences of Delayed Displacement Feedback Parameters. If there is only the delayed displacement feedback in (1), (14) becomes

$$\begin{aligned}\frac{2f\pi\omega}{\sqrt{2\alpha}}\operatorname{csch}\left(\frac{\pi\omega}{\sqrt{2k}}\right) > &\frac{2\sqrt{2}ck\sqrt{k}}{3\alpha}\\ &-\frac{\sqrt{2}ku}{2\alpha}\operatorname{csch}^2\left(\sqrt{\frac{k}{2}}\tau_1\right)\left[\sqrt{2k}\tau_1-\sinh\left(\sqrt{2k}\tau_1\right)\right].\end{aligned} \tag{15}$$

3.1.1. The Influence of Feedback Coefficient u. By the analysis of (15), we can find

$$\begin{aligned}&\operatorname{csch}^2\left(\sqrt{\frac{k}{2}}\tau_1\right) > 0,\\ &\lim_{\tau_1\to 0}\left[\sqrt{2k}\tau_1-\sinh\left(\sqrt{2k}\tau_1\right)\right]=0,\\ &\sqrt{2k}\tau_1-\sinh\left(\sqrt{2k}\tau_1\right)<0,\end{aligned} \tag{16}$$

so that

$$\begin{aligned}&-\frac{\sqrt{2}ku}{2\alpha}\operatorname{csch}^2\left(\sqrt{\frac{k}{2}}\tau_1\right)\left[\sqrt{2k}\tau_1-\sinh\left(\sqrt{2k}\tau_1\right)\right]\\ &>0.\end{aligned} \tag{17}$$

It could be found that the right-hand parts of (15) would become larger with the increasing of the delayed displacement feedback coefficient u. Accordingly, the critical excitation amplitude $f_{\min}$ for generating chaos will become larger with the increasing of u. In other words, the threshold value for chaotic motion in (1) will become larger, so that it is harder to generate chaos with larger u in (1).

In order to verify the validity of the analytical necessary condition for generating chaos, a set of illustrative system parameters is chosen as $k = 1$, $c = 0.4$, $\alpha = 1$, $\omega = 0.8$, and $\tau_1 = 0.5$. The numerical solutions for $f_{\min}$ of (1) are also investigated by numerical iterative method. When $u = 0.1$, the bifurcation diagram and the corresponding largest Lyapunov exponents are shown in Figures 1(a) and 1(b), respectively. The numerical simulation method for the largest Lyapunov exponents about delayed differential equation can be found in [38]. From the analysis of Figures 1(a) and 1(b), it could be found that the $f_{\min}$ values of generating chaos in two figures are consistent, which implies that the results by numerical iterative method are correct. Through the numerical simulation, the authors also observe some special dynamical phenomenon in this complex system. We find that there exist two paths leading to chaos via different period-doubling bifurcation in (1) which are shown in Figures 2(a) and 3(a), respectively. If the two paths are drawn on the same diagram which is shown in Figure 1, it could be found that the intersection point of the two paths is $f = 0.3774$. When $f < 0.3774$, there is a single periodic solution. If $f > 0.3774$, there will be two periodic-1 solutions, which depend on the initial values. The path shown in Figure 2(a) is simply named as "Type 1" and the other path shown in Figure 3(a) is "Type 2." In order to verify the conclusion, the time history, phase portrait, and Poincare maps at different typical points are presented and analyzed in the following part.

The transitions observed in Type 1 occur at $f \approx 0.3998$ ($1P \to 2P$) and 0.4040 ($2P \to 4P$), respectively. Some typical samples in different ranges are taken to analyze the dynamical phenomenon.

(1) When $f = 0.39$ and the initial value $[x_0, \dot{x}_0] = [-0.3956, 0.5858]$, the time history, phase portrait,

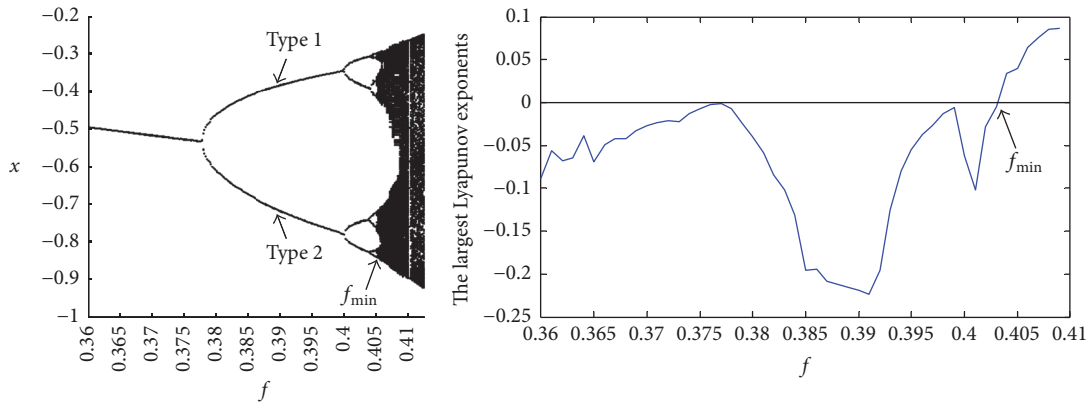

(a) Bifurcation diagram

(b) The largest Lyapunov exponents

FIGURE 1: The system responses for different excitation amplitude f.

and Poincare maps are shown in Figures 2(b1), 2(b2), and 2(b3), respectively. It could be found that it is period-1 motion in this case.

(2) When $f = 0.402$, the time history, phase portrait, and Poincare maps are shown in Figures 2(c1), 2(c2), and 2(c3), respectively. It is shown the dynamical motion is period-2 in this case.

(3) When $f = 0.4044$, the time history, phase portrait, and Poincare maps are shown in Figures 2(d1), 2(d2), and 2(d3), respectively. It could be found that it is period-4 motion in this case.

The transitions observed in Type 2 occur at $f \approx 0.4$ ($1P \to 2P$) and 0.4038 ($2P \to 4P$), respectively.

(1) When $f = 0.39$ and the initial value $[x_0, \dot{x}_0] = [-0.6, 0.5]$, the time history, phase portrait, and Poincare maps are shown in Figures 3(b1), 3(b2), and 3(b3), respectively. It could be found that the dynamical motion is period-1 in this case.

(2) When $f = 0.402$, the time history, phase portrait, and Poincare maps are shown in Figures 3(c1), 3(c2), and 3(c3), respectively. It could be found that it is period-2 motion in this case.

(3) When $f = 0.404$, the time history, phase portrait, and Poincare maps are shown in Figures 3(d1), 3(d2), and 3(d3), respectively. It could be found that the dynamical motion is period-4 in this case.

At last, f is selected as 0.41 and the initial values are selected randomly. It could be found that it is a chaotic motion in this case. The time history, phase portrait, and Poincare maps are shown in Figures 4(a), 4(b), and 4(c), respectively. Through the analysis of these dynamical characteristics at different typical points, the conclusion that there exist two paths leading to chaos in (1) can be proved.

If the same system parameters are substituted into (15), the relation curve of displacement feedback coefficient u and the critical excitation amplitude f_{min} could be got and shown in Figure 5 with solid line. According to the above numerical analysis process, the critical excitation amplitude f_{min} with different displacement feedback coefficient u could be found, and the relationship of u and f_{min} is also shown in Figure 5 with dots. From Figure 5, it could be found that the tendency of analytical results is similar to the numerical simulation. f_{min} will get smaller with the decreasing of u. That means the increase of u would make the threshold value for generating chaos of (1) larger. The larger u is able to prevent the generation of chaos.

3.1.2. The Influence of the Time Delay τ_1. From the analysis of (15), it could be found that it is an increasing function when $\tau_1 \in [0 \sim 1.5]$ and $-(\sqrt{2}ku/2\alpha)\text{csch}^2(\sqrt{k/2}\tau_1)[\sqrt{2k}\tau_1 - \sinh(\sqrt{2k}\tau_1)] > 0$. System typical parameters are chosen as $k = 1$, $c = 0.2$, $\alpha = 0.5$, $\omega = 1$, and $u = 0.01$, so that the relation curve of $\sqrt{k}\tau_1$ and f_{min} based on (15) is given in Figure 6 with solid line. The numerical results based on the above-mentioned numerical process are shown in Figure 6 with dots. From the observation of Figure 6, it could be obtained that increase of $\sqrt{k}\tau_1$ would make the threshold value for generating chaos larger, and it is against the generation of chaos.

3.2. The Influences of Delayed Velocity Feedback Parameters. If there is only the delayed velocity feedback in (1), (14) turns into

$$\sqrt{\frac{2}{\alpha}} f\pi\omega \,\text{sech}\left(\frac{\pi\omega}{2\sqrt{k}}\right) > \frac{4ck\sqrt{k}}{3\alpha} - \frac{2k\sqrt{k}v}{\alpha} \cdot \text{csch}^3\left(\sqrt{k}\tau_2\right) \cdot \left\{2\sinh\left(2\sqrt{k}\tau_2\right) - \sqrt{k}\tau_2\left[3 + \cosh\left(2\sqrt{k}\tau_2\right)\right]\right\}. \tag{18}$$

3.2.1. The Influence of Feedback Coefficient v. Here system typical parameters are chosen as $k = 1, c = 0.4, \alpha = 1, \omega = 0.8$, $\tau_2 = 0.5$ and v is chosen from 0 to 0.16. According to (18), the relation curve of v and f_{min} is obtained and shown in Figure 7

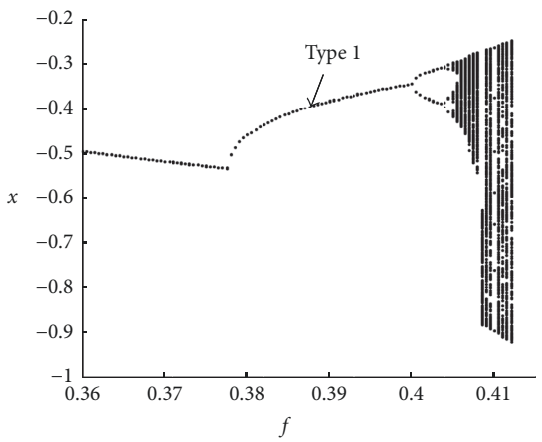

(a) Bifurcation diagram for Type 1

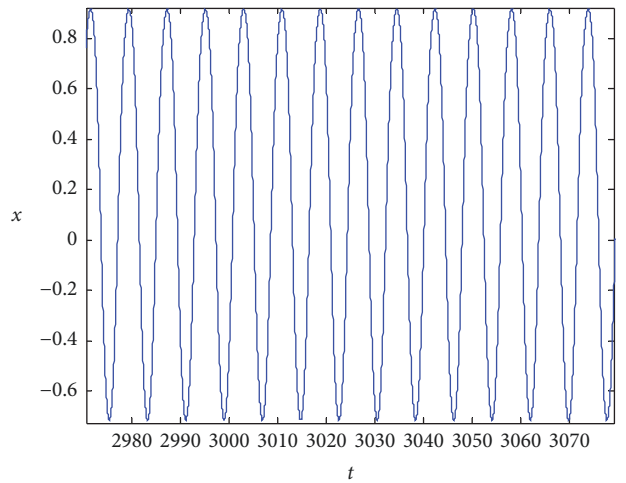

(b1)

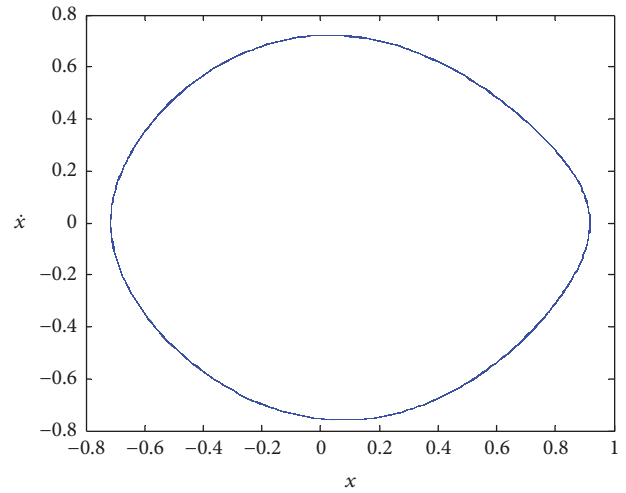

(b2)

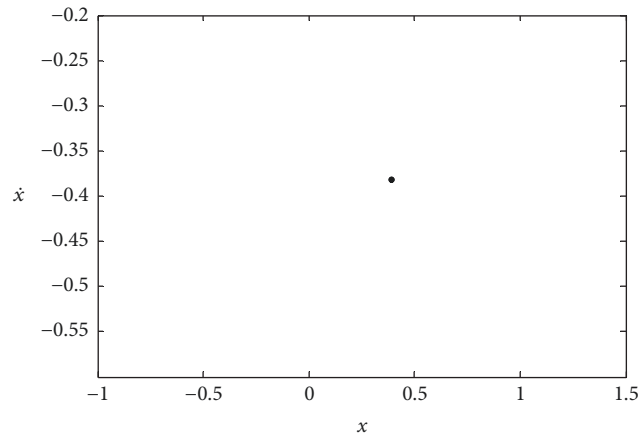

(b3)

(b) The system response at $f = 0.39$ for Type 1. (b1) Time history; (b2) phase portrait; (b3) Poincare maps

Figure 2: Continued.

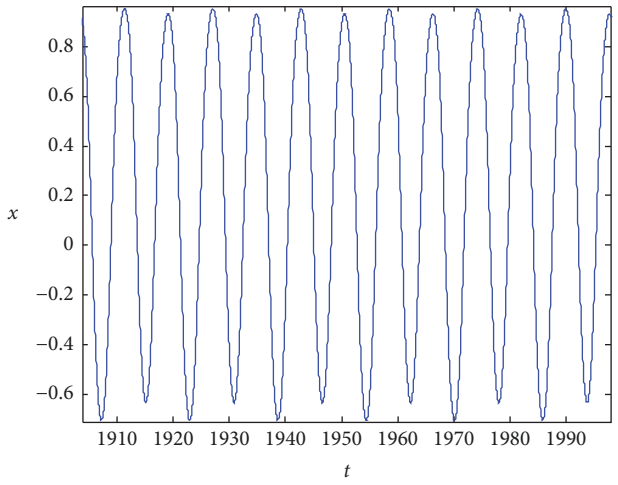

(c1)

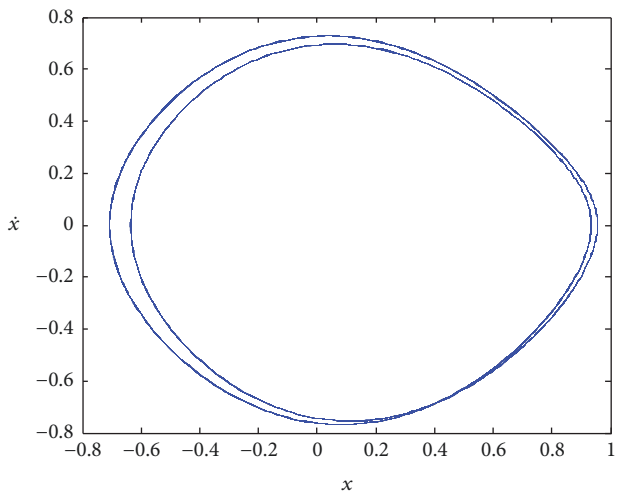

(c2)

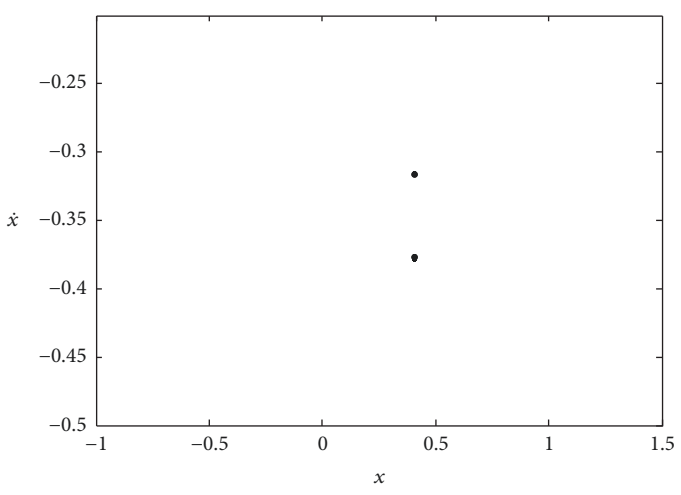

(c3)

(c) The system response at $f = 0.402$ for Type 1. (c1) Time history; (c2) phase portrait; (c3) Poincare maps

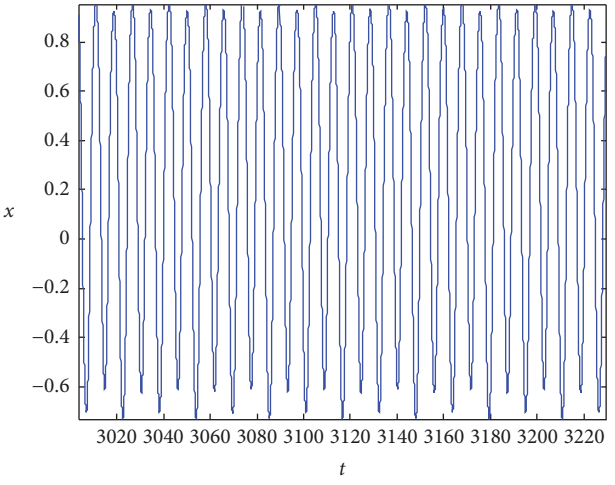

(d1)

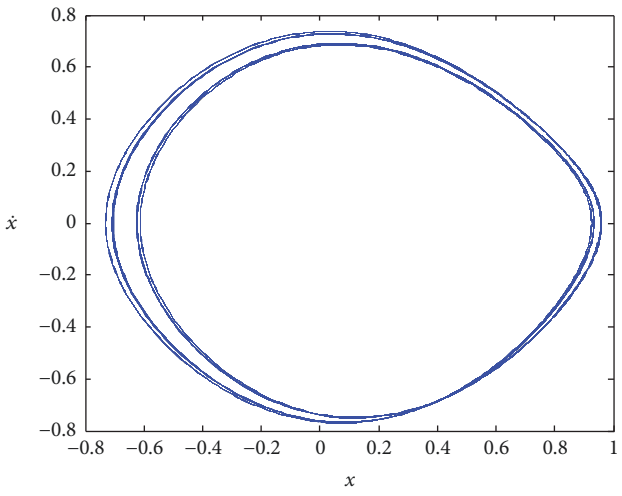

(d2)

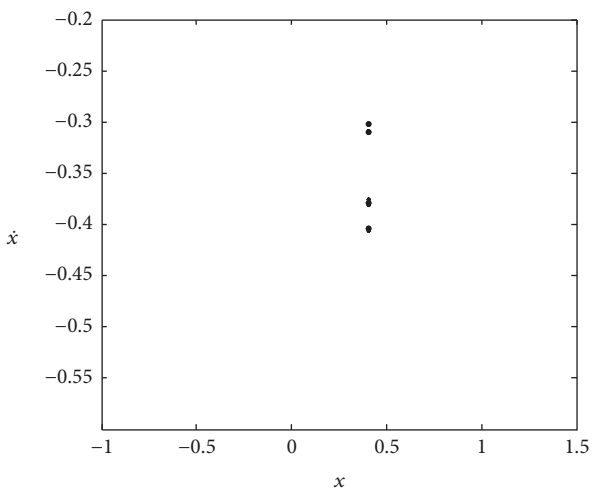

(d3)

(d) The system response at $f = 0.4044$ for Type 1. (d1) Time history; (d2) phase portrait; (d3) Poincare maps

Figure 2

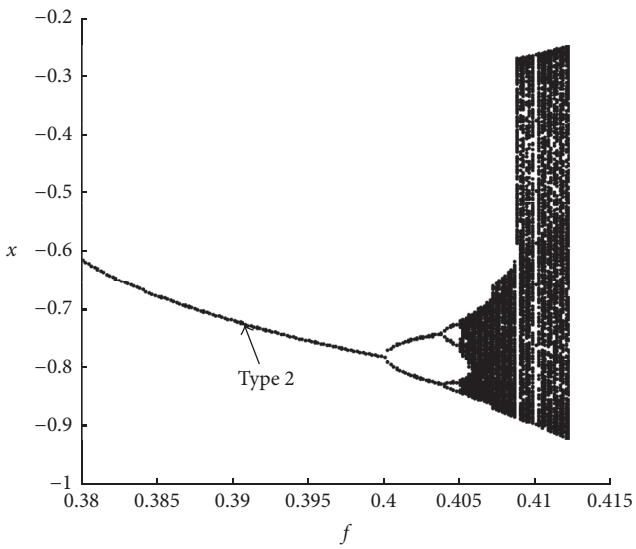

(a) Bifurcation diagram for Type 2

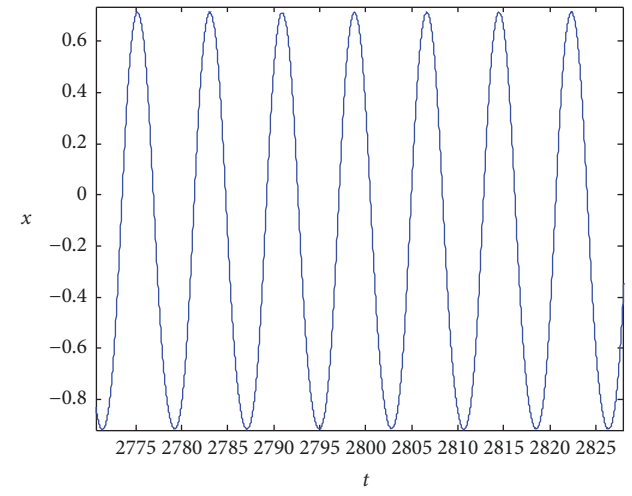

(b1)

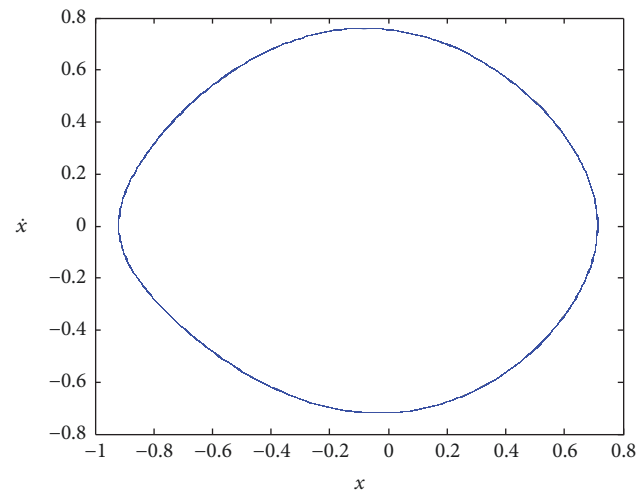

(b2)

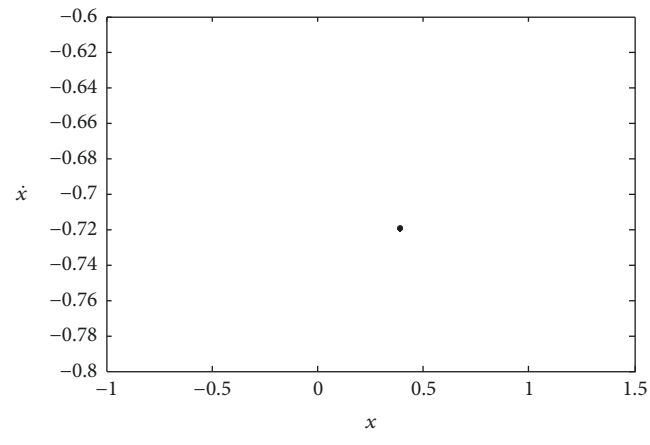

(b3)

(b) The system response at $f = 0.39$ for Type 2. (b1) Time history; (b2) phase portrait; (b3) Poincare maps

Figure 3: Continued.

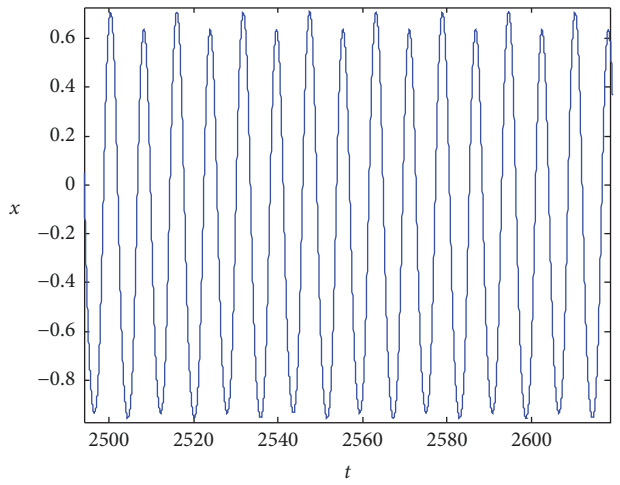

(c1)

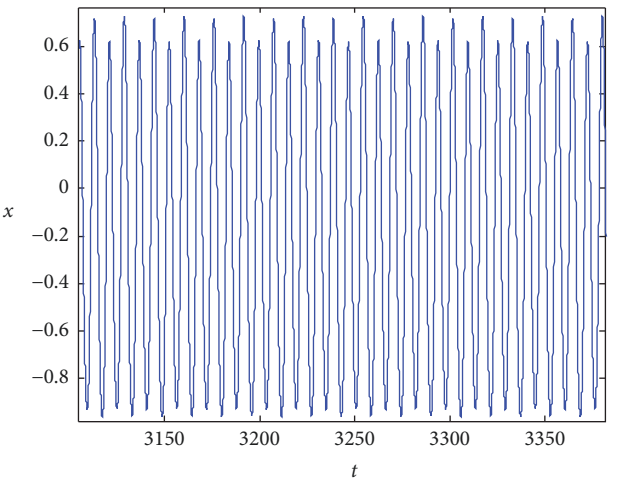

(d1)

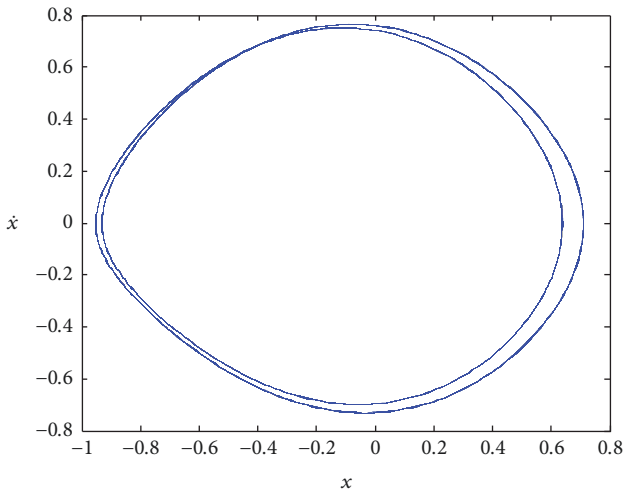

(c2)

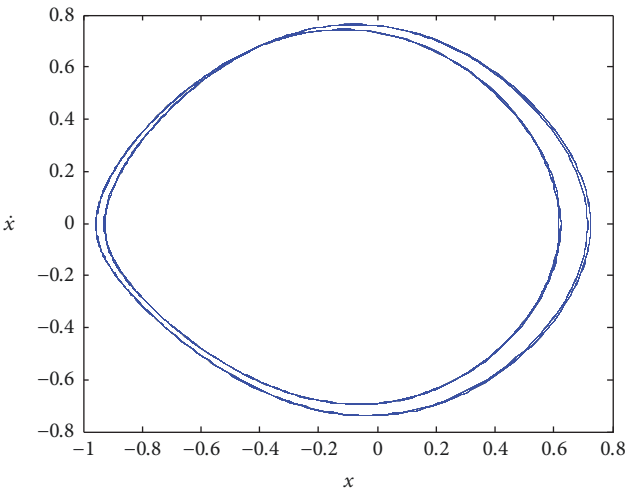

(d2)

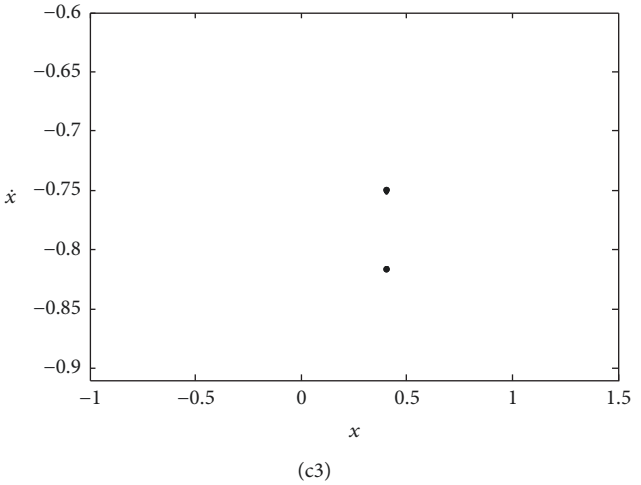

(c3)

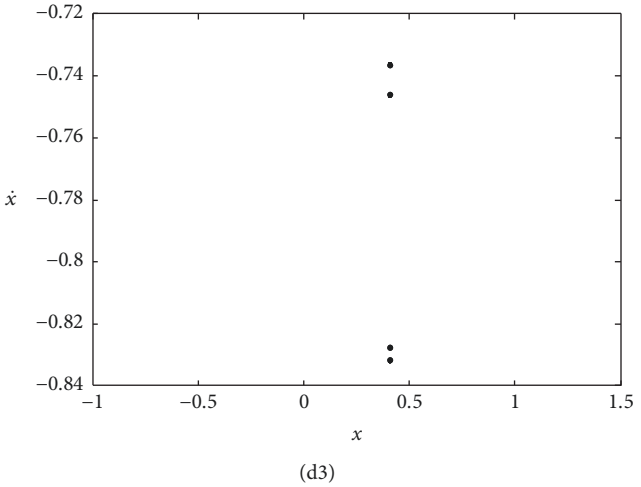

(d3)

(c) The system response at $f = 0.402$ for Type 2. (b1) Time history; (b2) phase portrait; (b3) Poincare maps

(d) The system response at $f = 0.404$ for Type 2. (b1) Time history; (b2) phase portrait; (b3) Poincare maps

Figure 3

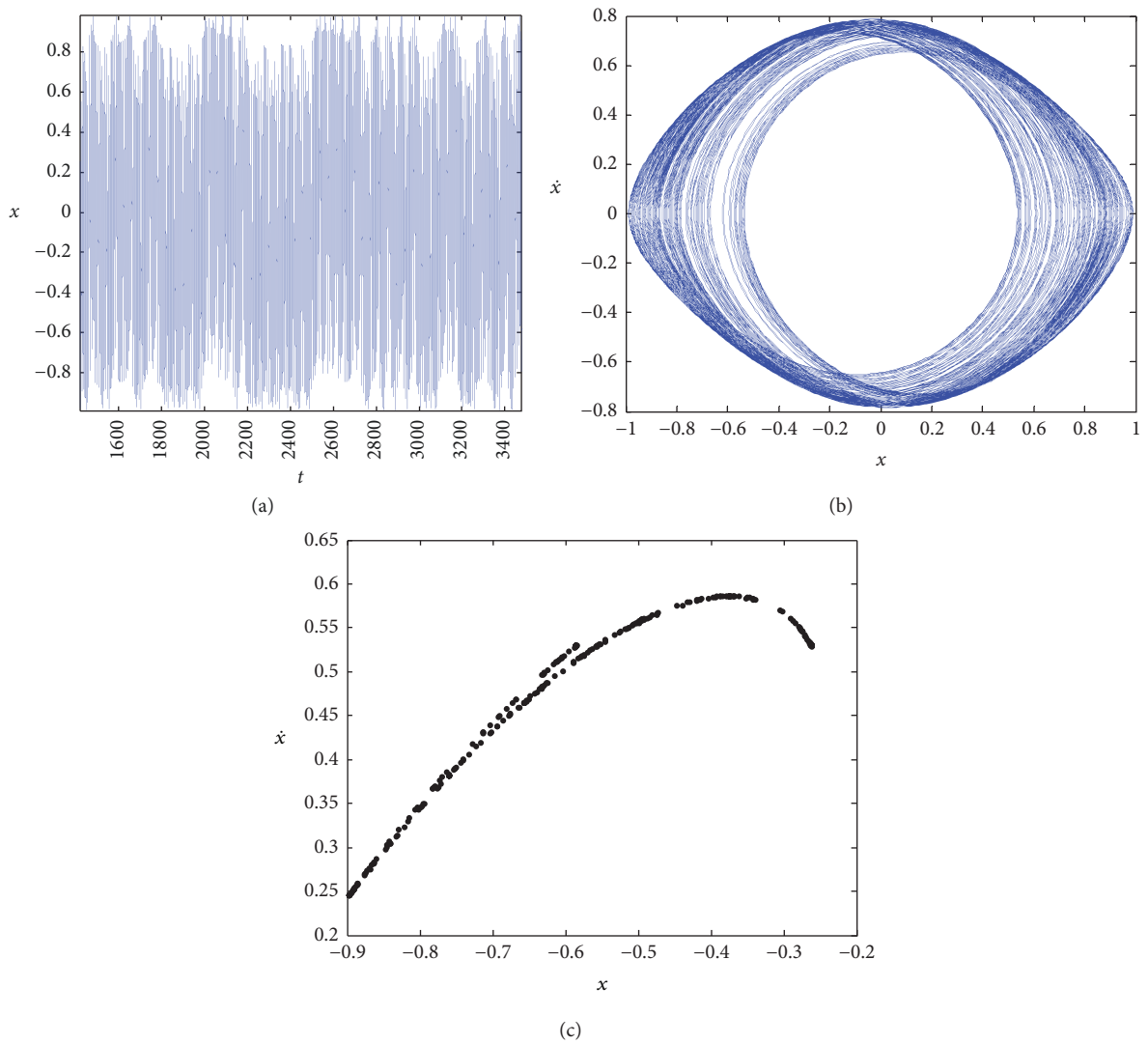

Figure 4: The system response at $f = 0.41$. (a) Time history; (b) phase portrait; (c) Poincare maps.

with solid line. The numerical simulation results based on the above-mentioned numerical method are shown in Figure 7 with dots. From the observation of Figure 7, it could be found that the increase of v would make the threshold value for generating chaos smaller, and it is beneficial to generate chaos.

3.2.2. The Influence of the Time Delay τ_2. The system parameters are chosen as $k = 1$, $c = 0.4$, $\alpha = 1$, $\omega = 0.8$, $v = 0.1$ and τ_2 is chosen from 0 to 0.16. According to (18), the relation curve of τ_2 and $f_{\min}$ is drawn in Figure 8 with solid line. The numerical simulation results are shown in Figure 8 with dots. From the observation of Figure 8, it could be found that the increase of τ_2 would make the threshold for generating chaos larger, and it is against generating chaos.

Through all the above analysis, it could be found that tendencies of the analytical solutions for the influences of all the delayed feedback parameters are consistent with the numerical iterative simulations. That is to say, a qualitative agreement between the numerical and analytical solutions is obtained. It is generally well known that the analytical necessary condition for the chaos in sense of Smale horseshoes by Melnikov method is the first-order approximate result, so that the quantitative differences between the numerical results and analytical solutions are acceptable. Although there are some differences of analytical solutions with numerical results, the conclusions of the analytical necessary condition for generating chaos are helpful to design this kind of delayed system or control the chaos by choosing appropriate system parameters.

4. Conclusion

In this paper, the heteroclinic bifurcation behavior of a Duffing oscillator under forcing excitation with both delayed

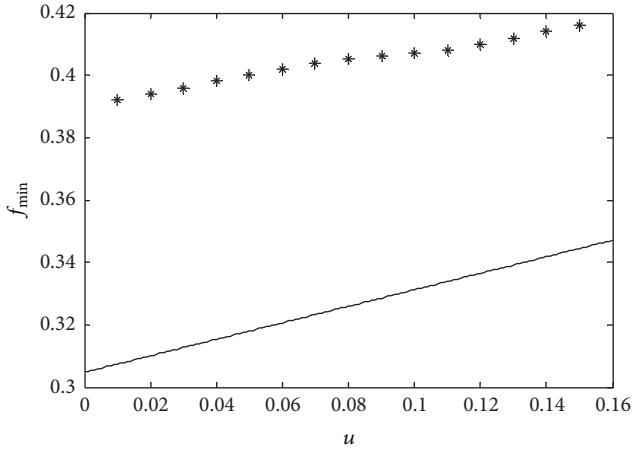

FIGURE 5: The relation curves of u and $f_{\min}$.

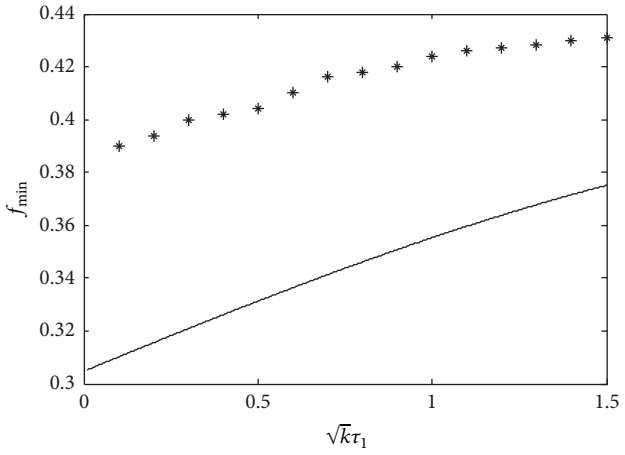

FIGURE 6: The relation curves of $\sqrt{k}\tau_1$ and $f_{\min}$.

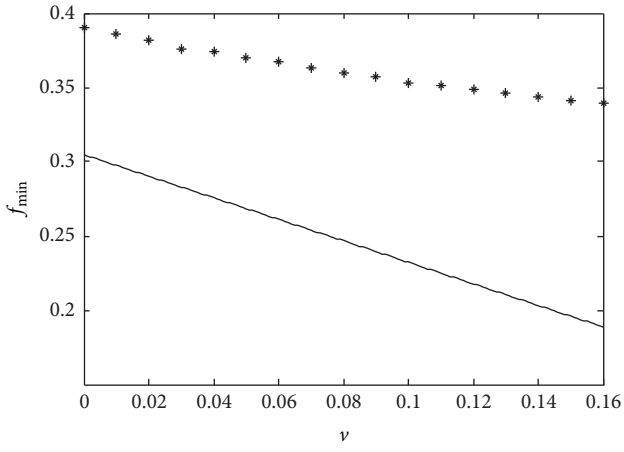

FIGURE 7: The relation curves of v and $f_{\min}$.

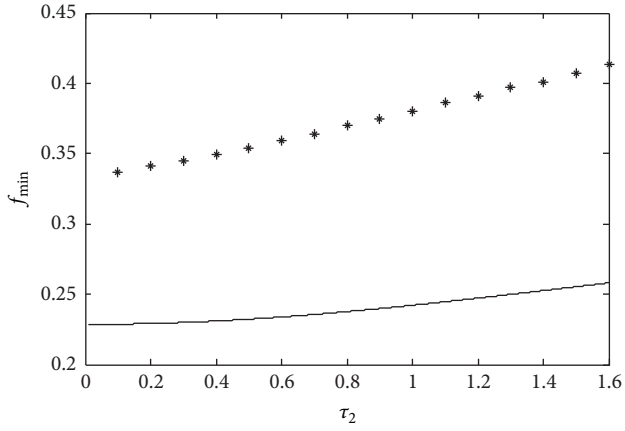

FIGURE 8: The relation curves of τ_2 and $f_{\min}$.

displacement feedback and delayed velocity feedback is investigated. The Melnikov function is established and the analytical necessary condition for generating chaos in (1) is obtained. The numerical simulation based on numerical iterative method is used to verify the correctness of the analytical necessary condition for generating chaos. The bifurcation and the large Lyapunov exponent figures are presented. From the analysis of numerical simulations, it could be found that two paths leading to chaos via period-doubling bifurcation exist in (1). The influences of the delayed feedback parameters are studied, respectively. From the analysis, we find that the tendencies of the analytical solutions for the influences of all the delayed feedback parameters are consistent with the numerical iterative simulations, which verifies the correctness of the analytical necessary condition. The systematic and comprehensive results are obtained. Those results will be helpful to design or control this kind of delayed feedback system.

Conflicts of Interest

The authors declare that they have no conflicts of interest.

Acknowledgments

The authors are grateful to the support by National Natural Science Foundation of China (no. 11602152 and no. 11272219) and the Education Department Project of Hebei Province (QN2016258).

References

[1] A. H. Nayfeh and D. T. Mook, *Nonlinear Oscillations*, John Wiley & Sons, New York, NY, USA, 1979.

[2] S. Yang and Y. Shen, "Recent advances in dynamics and control of hysteretic nonlinear systems," *Chaos, Solitons & Fractals*, vol. 40, no. 4, pp. 1808–1822, 2009.

[3] I. Kovacic and M. J. Brennan, "The Duffing Equation: Nonlinear Oscillators and their Behaviour," *The Duffing Equation: Nonlinear Oscillators and their Behaviour*, 2011.

[4] Y. Shen, S. Yang, and X. Liu, "Nonlinear dynamics of a spur gear pair with time-varying stiffness and backlash based on incremental harmonic balance method," *International Journal of Mechanical Sciences*, vol. 48, no. 11, pp. 1256–1263, 2006.

[5] X. Li, J. Hou, and Y. Shen, "Slow-fast effect and generation mechanism of Brusselator based on coordinate transformation," *Open Physics*, vol. 14, no. 1, pp. 261–268, 2016.

[6] Y.-J. Shen, L. Wang, S.-P. Yang, and G.-S. Gao, "Nonlinear dynamical analysis and parameters optimization of four semi-active on-off dynamic vibration absorbers," *Journal of Vibration and Control*, vol. 19, no. 1, pp. 143–160, 2013.

[7] H. Ding, "Periodic responses of a pulley-belt system with one-way clutch under inertia excitation," *Journal of Sound and Vibration*, vol. 353, pp. 308–326, 2015.

[8] Z. Jing and R. Wang, "Complex dynamics in Duffing system with two external forcings," *Chaos, Solitons & Fractals*, vol. 23, no. 2, pp. 399–411, 2005.

[9] Y. Shen, S. Yang, H. Xing, and H. Ma, "Primary resonance of Duffing oscillator with two kinds of fractional-order derivatives," *International Journal of Non-Linear Mechanics*, vol. 47, no. 9, pp. 975–983, 2012.

[10] Y. Shen, S. Yang, H. Xing, and G. Gao, "Primary resonance of Duffing oscillator with fractional-order derivative," *Communications in Nonlinear Science and Numerical Simulation*, vol. 17, no. 7, pp. 3092–3100, 2012.

[11] H. Y. Hu and Z. H. Wang, *Dynamics of Controlled Mechanical Systems with Delayed Feedback*, Springer Berlin Heidelberg, Berlin, 2002.

[12] Z. H. Wang and H. Y. Hu, "Stability switches of time-delayed dynamic systems with unknown parameters," *Journal of Sound and Vibration*, vol. 233, no. 2, pp. 215–233, 2000.

[13] Z.-M. Ge, C.-L. Hsiao, and Y.-S. Chen, "Nonlinear dynamics and chaos control for a time delay Duffing system," *International Journal of Nonlinear Sciences and Numerical Simulation*, vol. 6, no. 2, pp. 187–199, 2005.

[14] S. F. Wen, Y. J. Shen, and S. P. Yang, "Dynamical analysis of Duffing oscillator with fractional-order feedback with time delay," *Acta Physica Sinica*, vol. 65, Article ID 094502, 2016.

[15] A. C. J. Luo, "Time-Delayed Duffing Oscillator," in *Memorized Discrete Systems and Time-Delay*, pp. 271–296, Springer International Publishing, Switzerland, 2017.

[16] Y. A. Amer, A. T. EL-Sayed, and A. A. Kotb, "Nonlinear vibration and of the Duffing oscillator to parametric excitation with time delay feedback," *Nonlinear Dynamics*, vol. 85, no. 4, pp. 2497–2505, 2016.

[17] J. C. Ji and A. Y. T. Leung, "Bifurcation control of a parametrically excited Duffing system," *Nonlinear Dynamics*, vol. 27, no. 4, pp. 411–417, 2002.

[18] W. Zhang, M. H. Yao, and J. H. Zhang, "Using the extended Melnikov method to study the multi-pulse global bifurcations and chaos of a cantilever beam," *Journal of Sound and Vibration*, vol. 319, no. 1-2, pp. 541–569, 2009.

[19] S. Theodossiades and S. Natsiavas, "Non-linear dynamics of gear-pair systems with periodic stiffness and backlash," *Journal of Sound and Vibration*, vol. 229, no. 2, pp. 287–310, 2000.

[20] R. Van Dooren, "Comments on "non-linear dynamics of gear-pair systems with periodic stiffness and backlash"," *Journal of Sound and Vibration*, vol. 244, no. 5, pp. 899–903, 2001.

[21] R. Rusinek, A. Mitura, and J. Warminski, "Time delay Duffing's systems: Chaos and chatter control," *Meccanica*, vol. 49, no. 8, pp. 1869–1877, 2014.

[22] R. Rusinek, A. Weremczuk, K. Kecik, and J. Warminski, "Dynamics of a time delayed duffing oscillator," *International Journal of Non-Linear Mechanics*, vol. 65, pp. 98–106, 2014.

[23] B. R. Nana Nbendjo, R. Tchoukuegno, and P. Woafo, "Active control with delay of vibration and chaos in a double-well Duffing oscillator," *Chaos, Solitons & Fractals*, vol. 18, no. 2, pp. 345–353, 2003.

[24] T. Jiang, Z. Yang, and Z. Jing, "Bifurcations and chaos in the duffing equation with parametric excitation and single external forcing," *International Journal of Bifurcation and Chaos*, vol. 27, no. 8, Article ID 1750125, 2017.

[25] A. Sharma, V. Patidar, G. Purohit, and K. . Sud, "Effects on the bifurcation and chaos in forced Duffing oscillator due to nonlinear damping," *Communications in Nonlinear Science and Numerical Simulation*, vol. 17, no. 6, pp. 2254–2269, 2012.

[26] Y. Shi, "Melnikov analysis of chaos and heteroclinic bifurcation in Josephson system driven by an amplitude-modulated force," *International Journal of Dynamics and Control*, pp. 1-2, 2017.

[27] X.-L. Yang, W. Xu, and Z.-K. Sun, "Influence of harmonic and bounded noise excitations on chaotic motion of Duffing oscillator with homoclinic and heteroclinic orbits," *Wuli Xuebao/Acta Physica Sinica*, vol. 55, no. 4, pp. 1678–1686, 2006.

[28] Z. K. Sun, W. Xu, X. L. Yang, and T. Fang, "Inducing or suppressing chaos in a double-well Duffing oscillator by time delay feedback," *Chaos, Solitons & Fractals*, vol. 27, no. 3, pp. 705–714, 2006.

[29] M. S. Siewe, C. Tchawoua, and P. Woafo, "Melnikov chaos in a periodically driven Rayleigh-Duffing oscillator," *Mechanics Research Communications*, vol. 37, no. 4, pp. 363–368, 2010.

[30] Y. Y. Cao, K. W. Chung, and J. Xu, "A novel construction of homoclinic and heteroclinic orbits in nonlinear oscillators by a perturbation-incremental method," *Nonlinear Dynamics*, vol. 64, no. 3, pp. 221–236, 2011.

[31] Y. Chen and L. Yan, "Heteroclinic bifurcation analysis of Duffing-Van der pol system by the hyperbolic Lindstedt-Poincaré method," *Advanced Materials Research*, vol. 538-541, pp. 2654–2657, 2012.

[32] R. Chacon, "Melnikov method approach to control of homoclinic/heteroclinic chaos by weak harmonic excitations," *Philosophical Transactions of the Royal Society A: Mathematical, Physical & Engineering Sciences*, vol. 364, no. 1846, pp. 2335–2351, 2006.

[33] A. Maki, N. Umeda, and T. Ueta, "Melnikov integral formula for beam sea roll motion utilizing a non-Hamiltonian exact heteroclinic orbit: analytic extension and numerical validation," *Journal of Marine Science and Technology (Japan)*, vol. 19, no. 3, pp. 257–264, 2014.

[34] Y.-M. Lei and H.-X. Zhang, "Homoclinic and heteroclinic chaos in nonlinear systems driven by trichotomous noise," *Chinese Physics B*, vol. 26, no. 3, Article ID 030502, 2017.

[35] J. Guckenheimer and P. Holmes, *Nonlinear Oscillations, Dynamical Systems, and Bifurcation of Vector Fields*, Springer-Verlag, New York, NY, USA, 1983.

[36] P. J. Holmes, "A nonlinear oscillator with a strange attractor," *Philosophical Transactions of the Royal Society of London, Series A: Mathematical and Physical Sciences*, vol. 292, no. 1394, pp. 419–448, 1979.

[37] C. Cai, Z. Xu, and W. Xu, "Melnikov's analysis of time-delayed feedback control in chaotic dynamics," *IEEE Transactions on Circuits and Systems I: Fundamental Theory and Applications*, vol. 49, no. 12, pp. 1724–1728, 2002.

[38] J. C. Sprott, "A simple chaotic delay differential equation," *Physics Letters A*, vol. 366, no. 4-5, pp. 397–402, 2007.